Dynamic Contrast Enhanced (DCE) MRI-Derived Renal Perfusion and Filtration: Experimental Protocol

Pietro Irrera, Lorena Consolino, Walter Dastrù, Michael Pedersen, Frank G. Zöllner, and Dario Livio Longo

Abstract

Dynamic contrast-enhanced magnetic resonance imaging (DCE-MRI) can provide a noninvasive way for assessing renal functional information following the administration of a small molecular weight gadolinium-based contrast agent. This method may be useful for investigating renal perfusion and glomerular filtration rates of rodents in vivo under various experimental (patho)physiological conditions. Here we describe a step-by-step protocol for DCE-MRI studies in small animals providing practical notes on acquisition parameters, sequences, T_1 mapping approaches and procedures.

This chapters is based upon work from the COST Action PARENCHIMA, a community-driven network funded by the European Cooperation in Science and Technology (COST) program of the European Union, which aims to improve the reproducibility and standardization of renal MRI biomarkers. This experimental protocol chapter is complemented by two separate chapters describing the basic concept and data analysis.

Key words Magnetic resonance imaging (MRI), Kidney, Mice, Rats, Dynamic contrast-enhanced (DCE), Contrast agent, T_1 map

1 Introduction

Kidneys play an important role in fluid regulation, waste products elimination, and homeostasis of salts and pH. Therefore, accurate measurement of kidney function is essential for monitoring early renal injuries, disease progression, renal transplantation and in assessing therapeutic efficacy after renal failure [1, 2]. Magnetic resonance imaging (MRI) has emerged as a powerful technique that combines anatomical details with functional information. In recent years, various MRI techniques have been investigated for assessing renal function, including dynamic contrast-enhanced (DCE) MRI, arterial spin labelling (ASL), blood oxygenation level dependent (BOLD), diffusion weighted imaging (DWI), sodium imaging, chemical exchange saturation

transfer (CEST), and hyperpolarized MRI [3–9]. These techniques have shown promising results for the noninvasive evaluation of several renal function, including filtration, perfusion, oxygenation, pH, homeostasis, and others [10–27]. Among them, DCE-MRI or MR renography has emerged as a reliable method to reveal renal pathophysiology, functional and hemodynamic parameters. DCE-MRI relies on bolus administration of a gadolinium-based contrast agent (CA) [16], which changes the intrinsic longitudinal (T_1) and transversal (T_2) relaxation rates of protons in tissue. This means that administration of CA leads to an increased signal intensity on T_1-weighted images or decreased signal intensity on T_2-weighted images. DCE-MRI usually refers to T_1-weighted MR imaging techniques combined with a gadolinium-based CA using an acquisition scheme with a high temporal resolution. In the kidney the acquired signal over time leads to an MRI renogram, where the absolute signal intensity, in complex manner, depends on the native T_1 value, MRI sequence parameters, the specific magnetic relaxivity constant of the CA (the contrast agent efficiency, dependent also on its chemical structure [28–34]) and the concentration of the CA residing in the tissue [35, 36].

The main purpose of DCE-MRI is to reveal information about extravascular permeability, blood perfusion and compartmental kinetics. In practice, this method provides images prior and following the administration of the CA using a continuous image acquisition protocol. In kidneys, DCE-MRI is suitable for assessing kidney function in terms of filtration and perfusion [17]. Different post-processing methods allow estimations of kidney function and perfusion, either from simple semiquantitative approaches to more elaborated model-based analyses [37–42].

Here we describe step-by-step an experimental dynamic contrast enhanced (DCE) MRI protocol for monitoring the passage of a Gd-based tracer in the kidneys of rodents. The rationale for the choosing acquisition parameters is given in generic terms, together with specific parameter examples.

This experimental protocol chapter is complemented by two separate chapters describing the basic concepts and data analysis, which are part of this book.

This chapter is part of the book Pohlmann A, Niendorf T (eds) (2020) Preclinical MRI of the Kidney—Methods and Protocols. Springer, New York.

2   Materials

2.1   Animals

This experimental protocol was tailored for immune-competent (typically C57BL/6 and Balb/C) or immune-compromised (nude, NOD-SCID) mice with a body mass of 15–35 g. Advice for adaptation to rats is given as *Notes* where necessary. All animal

studies have to be carried out in compliance with specific legislation covering the use of animals for scientific purposes. Therefore, all experiments must be authorized under national regulations.

2.2 Lab Equipment and Chemicals

1. Mouse tail illuminator/restrainer for catheterizing the tail vein.

2. Saline solution or heparin solution, 1-ml syringe, catheter (e.g., PE 20 polyethylene tubing) of known inner diameter to hold the saline flush and for contrast agent bolus is required.

3. Anesthesia: please refer to the chapter by Kaucsar T et al. "Preparation and Monitoring of Small Animals in Renal MRI" for an in-depth description and discussion of the anesthesia. Typically, 0.5–1.5% isoflurane is used for anesthesia administered to the mice using an anesthetic gas vaporizer (Leica Biosystems, Maryland, USA). For nonrecovery experiments, urethane solution (Sigma–Aldrich, Steinheim, Germany; 20% in distilled water) can provide anesthesia for several hours with comparatively fewer side effects on renal physiology, which is an important issue. For intramuscular anesthesia, please refer to **Note 1**.

4. Gases: O_2, N_2, and compressed air, as well as a gas-mixing system or general inhalation anesthesia equipment, including an anesthetic vaporizer, a flow meter, and an induction chamber.

5. Mouse cradle.

6. Gd-based contrast agents: typically, small molecular weight FDA-approved gadolinium-based contrast agents are employed, such as gadoteridol (Prohance®, Bracco Imaging SpA, Milano, Italy), gadobutrol (Gadovist®, Bayer Healthcare Pharmaceuticals, Germany), or gadoteric acid (Dotarem®, Guerbert, France). Such clinically available contrast agents have stock concentrations of 0.5–1.0 mol/l that need to be diluted for handling volumes with less error (*see* **Note 2**).

7. Small animal ventilator: animals (rats) needs to be ventilated so the DCE-MRI acquisition can be gated to minimize the respiratory motion artifacts.

8. Syringe infusion pump: an MRI-compatible single syringe pump (Harvard Bioscience, Holliston, USA) for contrast agent administration for allowing precise timing infusion.

2.3 MRI Hardware

The general hardware requirements for renal 1H MRI on mice and rats are described in the chapter by Ramos Delgado P et al. "Hardware Considerations for Preclinical Magnetic Resonance of the Kidney." The technique described in this chapter was tailored for MRI preclinical systems at a magnetic field strength of 7 T but advice for adaptation to other magnetic field strengths is given where necessary (*see* **Note 3**). No special or additional hardware is required, except for the following:

1. A physiological monitoring system that can track the respiration and which is connected to the MRI system such that it can be used to synchronize DCE-MRI with respiration. Typically, we use an MRI-compatible rodent monitoring and gating system equipped with an air-pillow to monitor breath rate (Small Animal Instruments, New York, USA).

2.4 MRI Techniques   DCE-MRI experiments are performed by dynamic acquisitions of a strongly T_1-weighted imaging technique. The acquired signal following the CA administration is converted to relative concentrations of the gadolinium agent using either phantom calibration scales or by mathematical calculation of the sequence equation that describes the relationship between signal and MRI sequence parameters. The MRI sequence parameters, required volume coverage, spatial resolution, and SNR will determine the final temporal resolution. Several T_1 mapping approaches can be exploited for measuring the longitudinal relation times, a detailed description of different methods is provided in the chapter by Garteiser P et al. "Experimental Protocols for MRI Mapping of Renal T_1."

3 Methods

3.1 MR Protocol Setup

3.1.1 Variable Repetition Time (VTR) Acquisition for T_1 Mapping

1. Use a 2D RARE (rapid acquisition with refocused echoes) sequence with variable repetition times (RAREVTR on a Bruker MR system).

2. Set the acceleration factor (RARE-factor or echo train length, ETL) to at least 4 in order to shorten the acquisition time; an acceleration factor of 8–16 can be used to further shorten the acquisition time by sampling more k-space lines within a single repetition period (TR). Centric encoding can be exploited to minimize T_2 effects with increasing doses, but at the expenses or "blurred" images.

3. Set the echo time (TE) as short as possible for pure T_1-weight; in our setup an effective TE of 25 ms (defined by the acquisition of the central k-space line) was used.

4. Choose enough averages in order to have a sufficient signal to noise ratio (SNR) of above 30.

5. Repeat the RARE acquisition a number of times by changing the value of the repetition time (TR) to sample changes in signal intensities according to the expected T_1 values of the kidneys.

6. Because of the variability of the T_1 values inside the kidney regions, choose the TRs values to span a range large enough to permit an accurate calculation of T_1 by selecting 3–7 TR values in the range 100–10,000 ms (*see* **Note 4**).

7. For in vivo experiments, keep the overall acquisition time as short as possible by considering a trade-off between number of TRs, averages and matrix size (or spatial resolution).

8. For an example of a specific parameter set please *see* **Note 5**.

3.1.2 Variable Flip Angle (VFA) Acquisition for T_1 Mapping

1. Use a 2D gradient-echo sequence (FLASH on a Bruker system).

2. Set the echo time (TE) as short as possible for heavily T_1 weighting; in our setup a TE of 1.5 ms was used.

3. In order to have a sufficient signal to noise ratio, at least two averages have been acquired or enough averages for SNR > 30.

4. Repeat the FLASH acquisition a number of times by changing the value of the flip angle (FA). The changes in signal intensities will follow a parabolic curve, thus low flip angles and higher flip angles are needed to sample both side of this curve. Acquire a minimum of 2–3 flip angles, considering that experiments with more flip angles will improve the goodness of the T_1 estimate.

5. Set the TR in the range 10–100 ms for providing good T_1 weighting. Shorter TR increases T_1 weighting, but with detrimental SNR values; thus, a trade-off must be chosen, even considering number of averages and overall acquisition time.

6. For an example of a specific parameter set please *see* **Note 6**.

3.1.3 Fast Low Angle Shot (FLASH) T1-Weighted Sequence for DCE-MRI Experiments

1. Use a T_1-weighted sequence as a fast low angle shot (FLASH) sequence (in Bruker systems, this sequence refers to a dubbed FLASH sequence).

2. Use short TR to increase T_1-weighting, but this will decrease SNR. Therefore, a good balance should be found between strongly T_1-weighted images and image quality with sufficient SNR. Besides, TE and FA affect T_1-weighting and SNR. A good TR range could be between 5 and 100 ms (usually shorter values for 3D imaging and longer for 2D multislice acquisition).

3. Use the shortest echo time (TE) possible for pure T_1 weight.

4. Flip Angle (FA): high FA corresponds to a strong T_1 weighting, but at expenses of reduced SNR, therefore a good balance may result in FAs in the range 10–60°.

5. Use Partial Fourier acceleration to reduce the size of the acquired matrix and improve the time efficiency of data acquisition.

6. Use a high acquisition bandwidth (BW) to shorten TE, while keeping an eye on the SNR, which decreases with the square root of the increasing BW. For the image with the shortest TE an SNR of at least 30 is recommended.

7. Employ Fat Saturation modules. It is important to avoid fat signal overlaying with the kidney due to chemical shift.

8. Respiration trigger: there is no need to use respiratory triggering (per slice).

9. Adapt the geometry (or slice position) so that animal fits into FOV in Left-Right direction (approximately 30–40 mm according to the inner coil diameter) and use frequency encoding in Head-Feet direction. Use a slice with the lowest thickness the SNR allows, typically around 1–2 mm. The thinner the slices the better, as this improves the resolution which can be readily found on the raw images.

10. Use the highest in-plane resolution that the SNR allows, typically around 96×96 to 128×128 for FOV of 30×30 mm^2 or 40×40 mm^2. This resolution should be balanced by the need for sufficient SNR in the images. Zero-filling or use of partial Fourier techniques in the phase encoding direction can be helpful to speed up acquisition to minimize motion artifacts and contrast agent concentration changes during the acquisition. One may use half-Fourier acquisition schemes in read direction (asymmetric echo) to further shorten the TE. Reducing the excitation and refocusing pulse lengths to below 1.5 ms can then also help to shorten TE.

11. For an example of specific parameter sets for a 7 T MRI system, please *see* **Notes 7** and **8**, whereas for a scanner operating at 3 T please *see* **Note 9.**

3.2 Preparations of the Contrast Agent Injection and of the Catheter

1. Fill the 1-ml syringe with the contrast agent solution (*see* **Note 2**).

2. Prepare the catheter by filling the PE20 tubing with the contrast agent solution, and with 20–40 µl of a heparin solution (or a saline solution), between the needle (the animal) and the contrast agent solution to prevent clotting before the contrast agent will be injected.

3. According to the length of the catheter (usually 60–100 cm to exit from the magnet bore) the contrast agent solution can be injected directly from the syringe containing the contrast agent or by changing the syringe with one filled with a (heparin-free) saline solution for the postinjection flush.

3.3 Preparations of the Mouse

1. Place the mouse on a mouse tail illuminator restrainer for catheterizing the tail vein. The tail vein can be catheterized by placing a 27/29-G needle in the animal.

2. Induce anesthesia in animals via isoflurane in an induction box. Then transfer the animal to the MRI system (*see* **Note 10**).

3. Set up the temperature monitoring (rectal probe) and respiratory monitoring (balloon on chest) unit. During imaging, keep

the animal's respiration rate at 35–80 breaths per min by adjusting the dose of anesthesia (approximately 1–1.5% isoflurane with air and oxygen mixed at a 3:1 ratio administered through a nose cone attached to the animal bed and ophthalmic ointment will be applied to the eyes) (*see* **Note 11**).

4. Perform anatomical imaging as described in the chapter by Pohlmann A et al. "Essential Practical Steps for MRI of the Kidney in Experimental Research."

5. Since the AIF should be sampled with the same temporal resolution of the DCE-MRI experiment, selection of anatomical slices including large vessels near the kidneys should be considered.

6. Perform localized shimming on the kidney imaging as described in the chapter by Pohlmann A et al. "Essential Practical Steps for MRI of the Kidney in Experimental Research."

3.4   In Vivo T_1 Mapping

Typically, a T_1 map is acquired before the injection of Gd-based agent.

1. Select the same geometry of the anatomical images, with the same number of slices and position.

2. Load or select one of the several T_1 mapping sequences previously described (3.1). Adapt the same slice orientation as for the anatomical image with coronal or axial view with respect to the kidneys.

3. Run the T_1-mapping scan. Examples images are shown in Fig. 1 and Fig. 2.

3.4.1   DCE-MRI Experiment

1. Load the T_1-weighted sequence, adapt the slice orientation to provide a coronal or axial view with respect to the kidney (in scanner coordinates this is double-oblique) by importing the same geometry as for the anatomical (and T_1 mapping sequence).

2. Set the required number of repetitions accordingly to the sampling time and to the duration of the dynamic acquisition. Typically, 50–100 repetitions provide enough points to be exploited by any of the analysis procedures.

3. Initiate the DCE-MRI scan.

4. After some baseline image acquisition (5–10 images before the injection are enough to derive average baseline values and signal oscillations) perform an intravenous bolus injection of the Gd-based CA through the tail vein at a dose of 0.02–0.1 mmol Gd /kg b.w. by using a power injector to maintain the exact administration rate for each imaged mouse.

5. A demonstration of the signal intensity changes that can be expected for the DCE-MRI experiment across the kidneys is
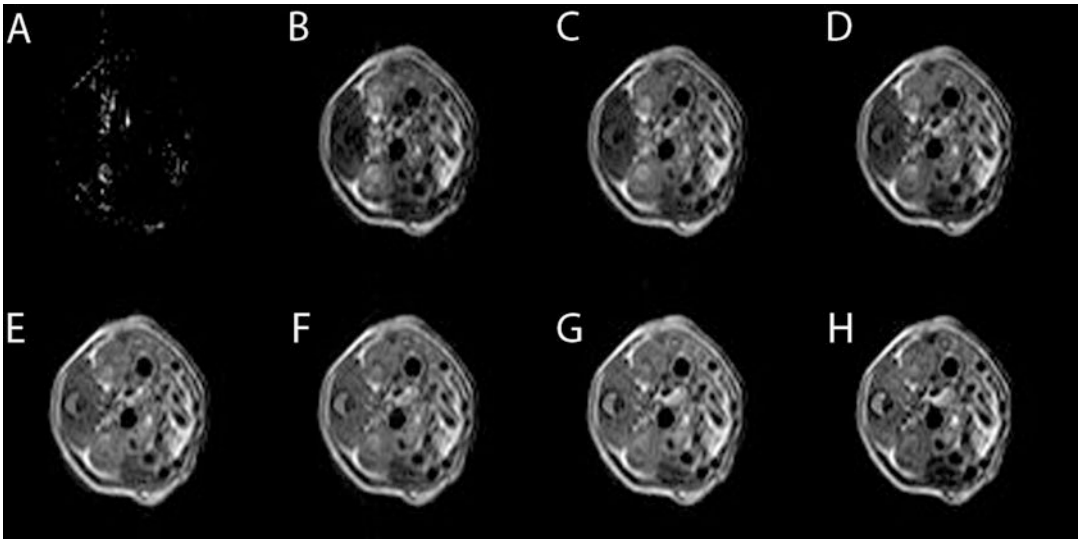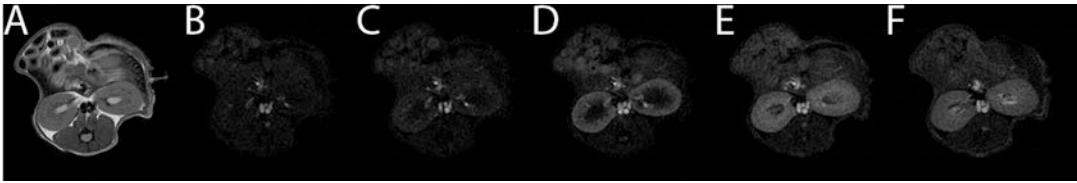
Fig. 1 Representative T_1-weighted images in kidneys obtained with the VTR scheme at different repetition times (TR) values: 75 ms (**a**), 534 ms (**b**), 1076 ms (**c**), 1738 ms (**d**), 2589 ms (**e**), 3782 ms (**f**), 5791 ms (**g**), and 15000 ms (**h**). Acquisition details are provided in **Note 5**
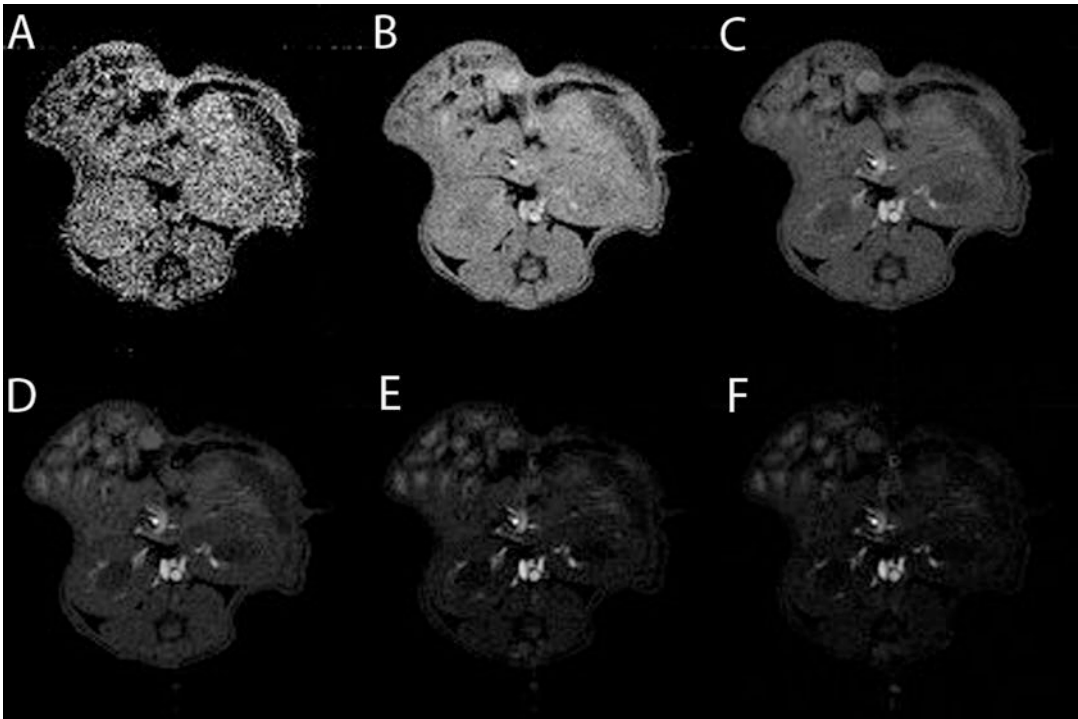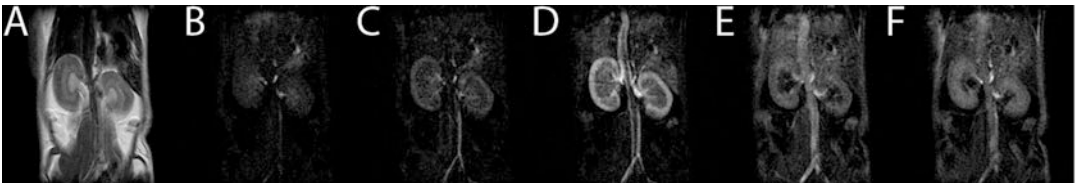

Fig. 2 Representative T_1-weighted images in kidneys obtained with VFA T_1 mapping approach by varying the excitation pulse flip angle values: 5° (**a**), 15° (**b**), 30° (**c**), 45° (**d**), 60° (**e**), and 75° (**f**) with a 7 T MRI system. Acquisition details are provided in **Note 6**

Fig. 3 Representative DCE-MRI images in kidneys (transversal orientation) at different time points following Gd-based contrast agent injection with a 7 T MRI scanner. Anatomical T_2-weighted (**a**) and GRE-FLASH T_1-weighted images before (**b**) and 4 s (**c**), 30 s (**d**), 5 min (**e**), and 10 min (**f**) after gadoteridol injection (dose 0.1 mmol Gd/kg b.w.). Acquisition details are provided in **Note 7**

Fig. 4 Representative DCE-MRI images in kidneys (coronal orientation) at different time points following Gd-based contrast agent injection with a 7 T MRI scanner. Anatomical T_2-weighted (**a**) and GRE-FLASH T_1-weighted images before (**b**) and 4 s (**bc**), 30 s (**d**), 5 min (**e**), and 10 min (**f**) after gadoteridol injection (dose 0.1 mmol Gd/kg b.w.). Acquisition details are provided in **Note 8**

given in Fig. 3 (axial orientation) and Fig. 4 (coronal orientation).

4 Notes

1. Intramuscular anesthesia can be administered as a mixture of xylazine 5 mg/kg (Rompun, Bayer, Italy) and tiletamine/zolepan 20 mg/kg (Zoletil 100, Virbac, Italy) with a dose dependent on the length of the MRI session. Usually, a 40–80 μl volume allows for a sleeping time of 30–60 min for a 25 g mouse.

2. A required dose for DCE-MRI in the kidneys is in the range 0.01–0.1 mmol Gd/kg b.w. that would require too small volumes of the stock solution. Therefore, it is advisable to dilute stock solutions to ca. 50 mmol/l. For instance, a 25 g mouse would receive 50 μl of 50 mmol/l Gd-complex to achieve a dose of 0.1 mmol Gd/kg. Please avoid the inclusion of air bubbles in the catheter filled with the saline solution or with the contrast agent solution that will be injected into the animals.

3. DCE-MRI experiments are described for Bruker MRI systems, such as Avance 300 (7 T) and Biospec (3 T), (Bruker, Ettlingen, Germany) or for a Magnetom Skyra 3 T (Siemens Healthcare, Erlangen, Germany). Standard ^{1}H radiofrequency-coils

(birdcage, quadrature) or phased-array ^{1}H coils can be used for data reception.

4. Within the Bruker method, specific TR values can be suggested according to the estimated T_1 values of the tissue.

5. For estimated T_1 of 1–3 s, 10 TR values can be used (580, 810, 1075, 1380, 1740, 2180, 2740, 3525, 4830, and 10,000 ms) to correctly follow signal intensities recovery until plateau. With 10 TR values complete acquisition lasted 8:40 min (for 96×96 matrix and 8 slices).

6. For estimated T_1 values of 1–3 s, we used six different FA values (5°, 15°, 30°, 45°, 60°, and 75°). With a TR of 80 ms and matrix size of 96×96, the single image acquisition lasted more than 15 s (8 slices). The complete acquisition time of the VFA T_1 map with six FA values is approximately 2 min.

7. Example for DCE-MRI using a FLASH readout at 7 T: TR: 16 ms; TE: 1.6 ms; FA: 30°; scan averages: 2; slice thickness: 1.5 mm; slice number: 1; slice orientation: axial; frequency encoding: head-feet; FOV $= 30 \times 30$ mm^2; matrix size $= 128 \times 128$; fat suppression $=$ on; acquisition time per image: 4 s; number of repetitions: 150.

8. Example for DCE-MRI using a FLASH readout at 7 T: TR: 15 ms; TE: 1.7 ms; FA: 30°; scan averages: 2; slice thickness: 1.5 mm; slice number: 1; slice orientation: coronal; frequency encoding: head-feet; FOV $= 30 \times 30$ mm^2; matrix size $= 128 \times 128$; fat suppression $=$ on; acquisition time per image: 4 s; number of repetitions: 150.

9. Example for DCE-MRI using a 3D time-resolved angiography with stochastic trajectories (TWIST) sequence at 3 T: TR $=$ 3.4 ms, TE $=$ 1.4 ms, FA: 20°, FOV $= 114 \times 50$ mm^2, generalized autocalibrating partially parallel acquisition (GRAPPA) of factor 2, matrix $= 192 \times 84$; slice number: 2, voxel resolution $= 0.6 \times 0.6 \times 1.2$ mm^3. TWIST view sharing: 15% central region, 20% sampling density in the outer region, nominal temporal resolution 0.9 s per volume. Images were continuously acquired for 6 min.

10. Mice can be alternatively anesthetized with intramuscular anesthesia, tail veins heated with hot water/heater equipment at 37 °C and catheter placed in the animal.

11. It is important to monitor the respiration continuously throughout the entire experiment.

Acknowledgments

References

1. Sawhney S, Mitchell M, Marks A, Fluck N, Black C (2015) Long-term prognosis after acute kidney injury (AKI): what is the role of baseline kidney function and recovery? A systematic review. BMJ Open 5(1):e006497. https://doi.org/10.1136/bmjopen-2014-006497

2. Joannidis M, Druml W, Forni LG, Groeneveld ABJ, Honore PM, Hoste E, Ostermann M, Oudemans-van Straaten HM, Schetz M (2017) Prevention of acute kidney injury and protection of renal function in the intensive care unit: update 2017: expert opinion of the Working Group on Prevention, AKI section, European Society of Intensive Care Medicine. Intensive Care Med 43(6):730–749. https://doi.org/10.1007/s00134-017-4832-y

3. Kline TL, Edwards ME, Garg I, Irazabal MV, Korfiatis P, Harris PC, King BF, Torres VE, Venkatesh SK, Erickson BJ (2018) Quantitative MRI of kidneys in renal disease. Abdom Radiol (NY) 43(3):629–638. https://doi.org/10.1007/s00261-017-1236-y

4. Zhang JL, Morrell G, Rusinek H, Sigmund EE, Chandarana H, Lerman LO, Prasad PV, Niles D, Artz N, Fain S, Vivier PH, Cheung AK, Lee VS (2014) New magnetic resonance imaging methods in nephrology. Kidney Int 85(4):768–778. https://doi.org/10.1038/ki.2013.361

5. Zhang JL, Rusinek H, Chandarana H, Lee VS (2013) Functional MRI of the kidneys. J Magn Reson Imaging 37(2):282–293. https://doi.org/10.1002/jmri.23717

6. Mannelli L, Maki JH, Osman SF, Chandarana H, Lomas DJ, Shuman WP, Linnau KF, Green DE, Laffi G, Moshiri M (2012) Noncontrast functional MRI of the kidneys. Curr Urol Rep 13(1):99–107. https://doi.org/10.1007/s11934-011-0229-6

7. Attenberger UI, Morelli JN, Schoenberg SO, Michaely HJ (2011) Assessment of the kidneys: magnetic resonance angiography, perfusion and diffusion. J Cardiovasc Magn Reson 13:70. https://doi.org/10.1186/1532-429X-13-70

8. Grenier N, Pedersen M, Hauger O (2006) Contrast agents for functional and cellular MRI of the kidney. Eur J Radiol 60(3):341–352. https://doi.org/10.1016/j.ejrad.2006.06.024

9. Ebrahimi B, Textor SC, Lerman LO (2014) Renal relevant radiology: renal functional magnetic resonance imaging. Clin J Am Soc Nephrol. https://doi.org/10.2215/CJN.02900313

10. Zollner FG, Konstandin S, Lommen J, Budjan J, Schoenberg SO, Schad LR, Haneder S (2016) Quantitative sodium MRI of kidney. NMR Biomed 29(2):197–205. https://doi.org/10.1002/nbm.3274

11. Zimmer F, Klotz S, Hoeger S, Yard BA, Kramer BK, Schad LR, Zollner FG (2017) Quantitative arterial spin labelling perfusion

measurements in rat models of renal transplantation and acute kidney injury at 3T. Z Med Phys 27(1):39–48. https://doi.org/10.1016/j.zemedi.2016.02.004

12. Hueper K, Peperhove M, Rong S, Gerstenberg J, Mengel M, Meier M, Gutberlet M, Tewes S, Barrmeyer A, Chen R, Haller H, Wacker F, Hartung D, Gueler F (2014) T1-mapping for assessment of ischemia-induced acute kidney injury and prediction of chronic kidney disease in mice. Eur Radiol 24(9):2252–2260. https://doi.org/10.1007/s00330-014-3250-6

13. Zollner FG, Schock-Kusch D, Backer S, Neudecker S, Gretz N, Schad LR (2013) Simultaneous measurement of kidney function by dynamic contrast enhanced MRI and FITC-sinistrin clearance in rats at 3 tesla: initial results. PLoS One 8(11):e79992. https://doi.org/10.1371/journal.pone.0079992

14. Hueper K, Rong S, Gutberlet M, Hartung D, Mengel M, Lu X, Haller H, Wacker F, Meier M, Gueler F (2013) T2 relaxation time and apparent diffusion coefficient for noninvasive assessment of renal pathology after acute kidney injury in mice: comparison with histopathology. Investig Radiol 48(12):834–842. https://doi.org/10.1097/RLI.0b013e31829d0414

15. Inoue T, Kozawa E, Okada H, Inukai K, Watanabe S, Kikuta T, Watanabe Y, Takenaka T, Katayama S, Tanaka J, Suzuki H (2011) Noninvasive evaluation of kidney hypoxia and fibrosis using magnetic resonance imaging. J Am Soc Nephrol 22 (8):1429–1434. https://doi.org/10.1681/ASN.2010111143

16. Notohamiprodjo M, Reiser MF, Sourbron SP (2010) Diffusion and perfusion of the kidney. Eur J Radiol 76(3):337–347. https://doi.org/10.1016/j.ejrad.2010.05.033

17. Sourbron SP, Michaely HJ, Reiser MF, Schoenberg SO (2008) MRI-measurement of perfusion and glomerular filtration in the human kidney with a separable compartment model. Investig Radiol 43(1):40–48. https://doi.org/10.1097/RLI.0b013e31815597c5

18. Prasad PV (2006) Evaluation of intra-renal oxygenation by BOLD MRI. Nephron Clin Pract 103(2):c58–c65. https://doi.org/10.1159/000090610

19. Dujardin M, Sourbron S, Luypaert R, Verbeelen D, Stadnik T (2005) Quantification of renal perfusion and function on a voxel-by-voxel basis: a feasibility study. Magn Reson Med 54(4):841–849. https://doi.org/10.1002/mrm.20608

20. Longo DL, Dastru W, Digilio G, Keupp J, Langereis S, Lanzardo S, Prestigio S, Steinbach O, Terreno E, Uggeri F, Aime S (2011) Iopamidol as a responsive MRI-chemical exchange saturation transfer contrast agent for pH mapping of kidneys: in vivo studies in mice at 7 T. Magn Reson Med 65(1):202–211. https://doi.org/10.1002/mrm.22608

21. Longo DL, Busato A, Lanzardo S, Antico F, Aime S (2013) Imaging the pH evolution of an acute kidney injury model by means of iopamidol, a MRI-CEST pH-responsive contrast agent. Magn Reson Med 70(3):859–864. https://doi.org/10.1002/mrm.24513

22. Longo DL, Sun PZ, Consolino L, Michelotti FC, Uggeri F, Aime S (2014) A general MRI-CEST ratiometric approach for pH imaging: demonstration of in vivo pH mapping with iobitridol. J Am Chem Soc 136 (41):14333–14336. https://doi.org/10.1021/ja5059313

23. Longo DL, Cutrin JC, Michelotti F, Irrera P, Aime S (2017) Noninvasive evaluation of renal pH homeostasis after ischemia reperfusion injury by CEST-MRI. NMR Biomed 30(7). https://doi.org/10.1002/nbm.3720

24. Longo D, Aime S (2017) Iodinated contrast media as pH-responsive CEST agents. In: Mcmahon MT, Gilad AA, JBM B, PCM VZ (eds) Chemical exchange saturation transfer imaging. Vol. Advances and applications. Pan Stanford Publishing, Singapore, pp 447–466. https://doi.org/10.1201/9781315364421-20

25. Wu Y, Zhou IY, Igarashi T, Longo DL, Aime S, Sun PZ (2018) A generalized ratiometric chemical exchange saturation transfer (CEST) MRI approach for mapping renal pH using iopamidol. Magn Reson Med 79 (3):1553–1558. https://doi.org/10.1002/mrm.26817

26. Mariager CO, Nielsen PM, Qi HY, Schroeder M, Bertelsen LB, Laustsen C (2017) Can hyperpolarized C-13-urea be used to assess glomerular filtration rate? A retrospective study. Tomography 3(3):146–152. https://doi.org/10.18383/j.tom.2017.00010

27. Duwel S, Hundshammer C, Gersch M, Feuerecker B, Steiger K, Buck A, Walch A, Haase A, Glaser SJ, Schwaiger M, Schilling F (2017) Imaging of pH in vivo using hyperpolarized (13)C-labelled zymonic acid. Nat Commun 8:15126. https://doi.org/10.1038/ncomms15126

28. Aime S, Botta M, Terreno E (2005) Gd(III)-based contrast agents for MRI. Adv Inorgan

Chem 57(57):173–237. https://doi.org/10.1016/S0898-8838(05)57004-1

29. Sherry AD, Caravan P, Lenkinski RE (2009) Primer on gadolinium chemistry. J Magn Reson Imaging 30(6):1240–1248. https://doi.org/10.1002/jmri.21966

30. Longo DL, Arena F, Consolino L, Minazzi P, Geninatti-Crich S, Giovenzana GB, Aime S (2016) Gd-AAZTA-MADEC, an improved blood pool agent for DCE-MRI studies on mice on 1 T scanners. Biomaterials 75:47–57. https://doi.org/10.1016/j.biomaterials.2015.10.012

31. Geninatti-Crich S, Szabo I, Alberti D, Longo D, Aime S (2011) MRI of cells and mice at 1 and 7 Tesla with Gd-targeting agents: when the low field is better! Contrast Media Mol Imaging 6(6):421–425. https://doi.org/10.1002/cmmi.436

32. Avedano S, Botta M, Haigh JS, Longo DL, Woods M (2013) Coupling fast water exchange to slow molecular tumbling in Gd3+ chelates: why faster is not always better. Inorg Chem 52 (15):8436–8450. https://doi.org/10.1021/ic400308a

33. Botta M, Avedano S, Giovenzana GB, Lombardi A, Longo D, Cassino C, Tei L, Aime S (2011) Relaxometric study of a series of monoaqua Gd-III complexes of rigidified EGTA-like chelators and their noncovalent interaction with human serum albumin. Eur J Inorg Chem 6:802–810. https://doi.org/10.1002/ejic.201001103

34. Botta M, Tei L (2012) Relaxivity enhancement in macromolecular and nanosized GdIII-based MRI contrast agents. Eur J Inorg Chem 12:1945–1960. https://doi.org/10.1002/ejic.201101305

35. Grenier N, Merville P, Combe C (2016) Radiologic imaging of the renal parenchyma structure and function. Nat Rev Nephrol 12 (6):348–359. https://doi.org/10.1038/nrneph.2016.44

36. Winter KS, Helck AD, Ingrisch M, Staehler M, Stief C, Sommer WH, Braunagel M, Kazmierczak PM, Reiser MF, Nikolaou K, Notohamiprodjo M (2014) Dynamic contrast-enhanced magnetic resonance imaging assessment of kidney function and renal masses: single slice versus whole organ/tumor. Investig Radiol 49(11):720–727. https://doi.org/10.1097/RLI.0000000000000075

37. Sourbron SP, Buckley DL (2013) Classic models for dynamic contrast-enhanced MRI. NMR Biomed 26(8):1004–1027. https://doi.org/10.1002/nbm.2940

38. Zollner FG, Daab M, Sourbron SP, Schad LR, Schoenberg SO, Weisser G (2016) An open source software for analysis of dynamic contrast enhanced magnetic resonance images: UMM-Perfusion revisited. BMC Med Imaging 16:7. https://doi.org/10.1186/s12880-016-0109-0

39. Beeman SC, Osei-Owusu P, Duan C, Engelbach J, Bretthorst GL, JJH A, Blumer KJ, Garbow JR (2015) Renal DCE-MRI model selection using Bayesian Probability Theory. Tomography 1(1):61–68. https://doi.org/10.18383/j.tom.2015.00133

40. Zollner FG, Zimmer F, Klotz S, Hoeger S, Schad LR (2014) Renal perfusion in acute kidney injury with DCE-MRI: deconvolution analysis versus two-compartment filtration model. Magn Reson Imaging 32(6):781–785. https://doi.org/10.1016/j.mri.2014.02.014

41. Zöllner FG, Zimmer F, Klotz S, Hoeger S, Schad LR (2015) Functional imaging of acute kidney injury at 3 Tesla: investigating multiple parameters using DCE-MRI and a two-compartment filtration model. Z Med Phys 25(1):58–65. https://doi.org/10.1016/j.zemedi.2014.01.002

42. Zollner FG, Weisser G, Reich M, Kaiser S, Schoenberg SO, Sourbron SP, Schad LR (2013) UMMPerfusion: an open source software tool towards quantitative MRI perfusion analysis in clinical routine. J Digit Imaging 26 (2):344–352. https://doi.org/10.1007/s10278-012-9510-6